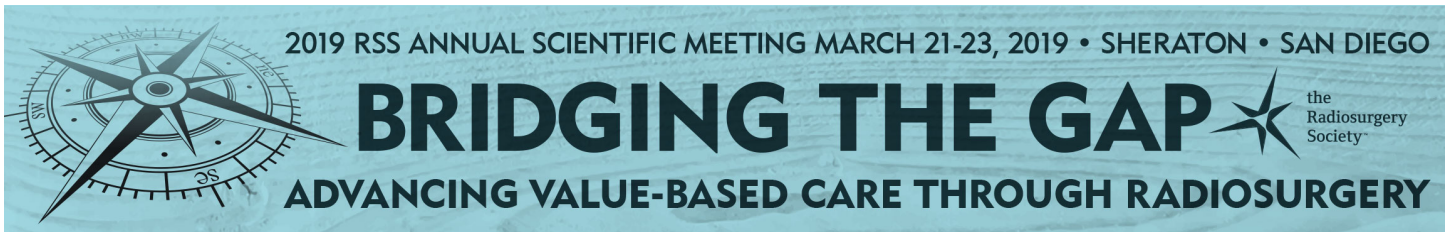

PHYSICS SESSION ABSTRACTS

Real-Time Target Tracking in Pancreatic SBRT: Characterizing the Clinical Impact

Bernard L Jones, Karyn A Goodman, Tracey Schefter, Moyed Miften, and Yevgeniy Vinogradskiy

Objectives: Abdominal motion can increase the risk of toxicity and hinder dose-escalation in Stereotactic Body Radiotherapy (SBRT) of pancreatic tumors. Real-time imaging and tracking is an emerging technique to increase the accuracy of delivery. We report on a large, retrospective cohort of pancreatic patients treated with real-time, fiducial-based kV image guidance. The purpose of our study was to determine the clinical and dosimetric impact of real-time target tracking in pancreatic SBRT by answering three key clinical questions: what is the impact of real-time target tracking on 1) clinical workflow, 2) treatment accuracy, and 3) tumor dose? To answer these questions, we retrospectively analyzed data collected during pancreatic SBRT with real-time target tracking.

Methods: 68 patients were treated with pancreatic SBRT under real-time kV image guidance. kV images were acquired during treatment to visualize the location of implanted fiducial markers. Corrections were made to the position if the markers were observed >3 mm from the expected reference position. To understand impact on treatment accuracy and clinical workflow, we retrospectively analyzed all treatment interruptions and corrections made based on this imaging. To assess the dosimetric impact of the real-time imaging, an artificial neural network dosimetric model was trained with prior clinical plans to calculate the impact of real-time imaging interventions on tumor dose.

Results: Real-time imaging resulted in 0.81 pauses per fraction of treatment. 60% of the treatment pauses were due to having to adjust the gating thresholds and 40% were due to having to re-localize the target. The average time per pause was 1.9 ± 1.8 minutes. Treatment pauses that required patient re-alignment due to real-time tumor tracking occurred during 32% of all fractions. The median shifts for patient re-alignment were 0.8 mm (AP), 4.0 mm (SI), and 1.2 mm (LR). The median radial (3D) shift was 5.2 mm. 41% of all patients had at least one shift throughout the course of treatment with magnitude >5 mm, and 16% of all fractions had at least one treatment pause that required an alignment >5 mm. 45% of shifts resulted in dosimetric differences to the tumor; of these, the median point dose difference was 23% ± 22% of prescription dose (max 94%). The number of pauses per fraction was significantly higher in patients treated with respiratory gating (vs. abdominal compression) and in patients with greater treatment time.

Conclusions: In this study, we demonstrated the feasibility of fiducial-based real-time target tracking for pancreatic SBRT treatment, and quantified the benefits of this imaging to increase the accuracy of pancreatic SBRT. This dataset represents, to our knowledge, the largest experience treating these tumors with fiducial marker-guided in-treatment kV imaging. Our data indicate that real-time tumor tracking leads to patient re-alignment in 32% of cases and results in significant dosimetric benefit to target coverage. The increased accuracy of real-time target tracking may potentially enable safe dose escalation in pancreatic SBRT.

Determination of Treatment Margins for Head and Neck Tumors Treated with a Robotic Radiosurgery System Using Spine or Skull Tracking

Justin Hurley, MS, Michael May, MD, Neal Dunlap, MD,
Brian Wang, PhD, Joshua James, MS

Objectives: Robotic radiosurgery relies on imaging of fiducial markers, bony anatomy, or in some lung cases the tumor itself, to localize the target volume at the time of treatment. When using bony anatomy as a surrogate to localize soft tissue targets, there is an uncertainty in the localization of the target itself due to positional changes relative to the bony anatomy being tracked. The two purposes of this study are: (1) determine whether the spine or skull is a better bony anatomy surrogate depending on the location of the tumor; and (2) quantify the required treatment margins for head and neck tumors when aligning to the spine or skull.

Methods: A retrospective study of 16 head and neck cancer patients treated with stereotactic body radiation therapy (SBRT) on gantry-based linear accelerators was done by collecting data from 81 daily cone-beam computed tomography (CBCT) images. At the time of treatment, each CBCT was aligned to the reference planning CT based on tumor position. Using the Offline Review module in Aria version 11, rigid registrations were performed to realign the daily CBCT to the reference planning CT using both the spine and skull, separately, as the basis of the registration. Shifts from the treatment position to the new positions in the vertical, lateral and longitudinal dimensions were recorded. The magnitude of the shifts and the location of the tumor were used to classify each patient into the most appropriate tracking method (spine or skull), and the data were stratified accordingly. The margins needed to adequately cover the treatment volume with the 95% isodose surface for 90% of the patient population were calculated based on van Herk's margin recipe using the per patient mean and standard deviations of the shifts in each dimension.

Results: When the superior border of the tumor was located above the C1 vertebra, aligning to the skull required an average 1.0 mm smaller total shift compared to aligning to the spine. All other tumors had an average 1.0 mm smaller total shift when aligning to the spine; therefore, superior tumor extent was used to classify patients. When using spine tracking, a margin of 3.0 mm, 2.7 mm and 0.17 mm was calculated in the vertical, longitudinal and lateral dimensions, respectively. When using skull tracking, a margin of 1.5 mm, 1.7 mm and 1.7 mm was calculated in the vertical, longitudinal and lateral dimensions, respectively.

Conclusions: An additional margin is needed to account for uncertainties in head and neck tumor location when the spine or skull is used as a surrogate for patient positioning during robotic radiosurgery. For patients with tumor extent superior to the C1 vertebra, we recommend using skull tracking with a uniform 2 mm margin; and for patients with the entire tumor at the C1 vertebra and inferior, we recommend using spine tracking with a uniform 3 mm margin.

Dose Discrepancy of External SRS Audit - Investigation of Linac Deliverability Factors

Kirsty Blythe, Savvas Rizkalla, Tony Greener

Objectives: As part of commissioning of TrueBeam STx for use in intracranial Stereotactic RadioSurgery, in November 2016 Guys and St Thomas NHS Foundation Trust took part in a UK Cranial Stereotactic Radiosurgery Dosimetry Audit. The measured results across a number of alanine pellets within the planning target volume of an anthropomorphic phantom were +5% higher than predicted values from Eclipse. This study aimed to validate this result using several small chambers and phantoms, and to investigate possible machine deliverability factors which may have contributed to the discrepancy.

Methods: Five different plans of increasing complexity (1. Simple 10x10 square fields, 2. Prostate VMAT 3. Neuro VMAT 4, SBRT Lung VMAT 5. NPL Audit SRS non-coplanar SRS VMAT plan) and range of energies (6X, 10FFF) were measured with four different measurement setups (1. A1SL Chamber inside STEEV phantom, 2. SemiFlex Chamber inside STEEV phantom, 3. SemiFlex3D Chamber inside STEEV phantom, 4. A1SL using CHEESE phantom).

All chambers were cross calibrated using two methods, a side by side method in a Perspex block and by chamber exchange method in a water phantom.

Results: After initial cross calibration of the SemiFlex 3D chamber, it was found to give results of +3.2% for 10x10cm 10FFF orthogonal fields in the STEEV phantom. Despite repeated cross calibrations the SemiFlex3D chamber continued to over-respond for all subsequent setups and these results have been disregarded.

Otherwise, 10x10cm orthogonal fields with all phantom and chamber combinations at 6MV and 10FFF agreed within 1% of predicted values for remaining chambers and setups. The prostate VMAT plan agreed within 2.5% for the SemiFlex chamber and within 2% for the A1SL chamber in STEEV and within 1% for the A1SL in CHEESE. The more complex neuro VMAT plan agreed within 3% for both chambers in STEEV and within 1.5% in CHEESE. A SBRT Lung VMAT plan agreed within 3% in STEEV and 1.3% in CHEESE using both SemiFlex and A1SL chambers.

The SRS audit plan was measured as +3% high in STEEV with the A1SL chamber and SemiFlex chamber. This is 2% lower than as measured during the audit, which used the same phantom but different detectors (alanine pellets). This plan measured +1.3% using the A1SL chamber in the CHEESE phantom, which may be due to the greater homogeneity of this phantom.

Conclusions: Agreement between expected doses and measured doses may worsen with increasing plan complexity (MU/Gy). The dose per fraction also increased in these cases from 2Gy/# (Prostate VMAT) up to 24Gy/# (SRS VMAT). Further audit visits were carried out and DLG has been considered to be influential in this dose discrepancy. Further work is required to identify what elements in the plans contribute to worse agreement between planning system and measurement. A study was conducted which evaluated planning parameters by making systematic adjustments to the audit plan in Eclipse, and is reported on in a separate abstract.

Determining the Spatial Accuracy of Frameless Linac-Based Radiosurgery for Trigeminal Neuralgia

Daphne Levin, Efrat Shekel, **Dan Epstein**

Objectives: To determine the spatial accuracy of frameless linac-based radiosurgery for trigeminal neuralgia.

Methods: We used two different phantoms to measure spatial and dosimetric accuracy of a frameless SRS treatment for trigeminal neuralgia. The first phantom was created using a 3D printer to construct an anatomically accurate hollow phantom using a patient's DICOM images. The phantom was filled with a polymer gel dosimeter. The gel's characteristics are such that it changes its chemical behavior in proportion to the dose absorbed. These changes can be detected under specific MRI sequences. The actual patient treatment plan, consisting of 7 non-coplanar arcs and delivered with a 4 mm cone, was irradiated onto the phantom. We molded an SRS mask for the phantom, and used a kV-kV positioning system to verify positioning between arcs. The phantom was subsequently scanned by MRI using predefined pulse sequences to generate high spatial resolution 3D T2 maps. These maps were then converted into 3D dose distribution measurements that were co-registered to the real patient planning CT images, RT structures, and TPS calculated dose data.

The second phantom was a commercial SRS head phantom with accurate bony anatomy and interchangeable inserts for diodes, ion chambers and films. We irradiated this phantom with the same plan, once using a diode for total dose measurement, and once with high dose (up to 100 Gy) gafchromic film for spatial resolution.

Results: For the 3D phantom, relative dose profiles through the target volume for measured and TPS-calculated datasets were compared. Our results showed an agreement of better than 1mm throughout the various profiles.

2D gamma comparisons were also performed with passing criteria of 2mm distance to agreement and 5% dose difference for selected slices of the phantom. We obtained better than 98% pass rate on all slices.

DVH comparisons for planned and measured relative dose distributions for PTV and trigeminal nerve were calculated. Doses were normalized to 100% corresponding to the dose received by at least 50% of the volume for each structure. Mean PTV dose was 98% vs 97% for TPS vs measured dose and D95% was 16% for both measured and TPS dose for the trigeminal nerve.

For the second phantom we achieved a dose accuracy of 2%, and a spatial accuracy of 0.4mm.

Conclusions: Frameless linac-based radiosurgery with a 4 mm cone can be highly spatially accurate if delivered carefully, with use of appropriate imaging between arcs. End-to-end verification of accuracy is necessary to ensure quality of treatment at least as part of implementation of a high dose, high accuracy SRS program.

Comparison of Surrogate Matching Methods for Target Localization with Free-Breathing in Stereotactic Body Radiation Treatment for Liver Tumors

Shiby Paul, Shu-Hui Hsu, Christian Velten, Nitin Ohri, Rafi Kabarriti, Wolfgang Tome, Shalom Kalnicki, Madhur Garg

Objectives: The use of fiducials implanted around liver tumors or lipiodol present in transarterial chemoembolization cavities allow for accurate target positioning during stereotactic body radiation therapy (SBRT) for liver tumors. Other markers such as calcifications, stents, and surgical clips that are in close proximity to the target volume aid in daily patient setup. A majority of patients, however, have no such, or unusable markers. The present study investigates the 3D image matching accuracy between the planning computed tomography (CT) and daily pretreatment 3D cone beam computed tomography (CBCT) based on the anatomical surrogates bone (spine), liver, and diaphragm in free-breathing SBRT.

Methods: We identified patients treated with free breathing liver SBRT at our institution having markers including fiducials, lipiodol, stents, clips or calcifications, with none of them further than 3 cm away from the target volume. Patients were immobilized with Elekta blueBAG™ with vacuum coversheet. Those with respiratory motion in excess of 15 mm in any direction on acquired 4D-CTs were excluded. The planning CTs were retrospectively registered to the pretreatment CBCTs based on markers, liver, bony anatomy, and diaphragm using rigid registration. The coordinates for marker registration were used as reference coordinates. Differences of registration coordinates between the marker and liver/diaphragm/bone registrations were used to quantify target positioning error. Statistical significance between all the registrations was assessed using t-tests in craniocaudal (C-C), mediolateral (M-L), anteroposterior (A-P) direction. Planning target volume (PTV) margin estimates were calculated using Van Herk formula.

Results: Thirty-four CBCTs from seven patients who met the eligibility criteria treated during 2015-2018 were used for the analysis. Six patients had hepatocellular carcinoma and one had metastatic sigmoid adenocarcinoma. Three patients were treated to segment 7, two to segment 8 and one each to segments 2 and 5. Lipiodol was the marker in 15, calcifications in 10, and clips in 9 out of 34 CBCTs. The 3D positioning error compared to markers was the smallest when using liver matching (3.0 ± 0.3 mm), followed by diaphragm (3.6 ± 0.3 mm) and bone (4.5 ± 0.4 mm) matching, with all $p < 0.05$. Absolute positioning errors were significantly lower in C-C direction with liver and diaphragm matching compared to bone matching ($p < 0.05$). In M-L direction the positioning errors were significantly lower with liver matching compared to bone matching ($p < 0.05$) and there was a trend to lower error in A-P direction with liver compared to bone as well as in M-L direction with diaphragm matching compared to bone. Liver matching had the lowest interfraction error with a magnitude of 2.0 ± 0.3 mm compared to 2.5 ± 0.3 mm and 2.7 ± 0.3 mm for diaphragm and bone matching, respectively. We estimate image registration-based target positioning error contribution to PTV margins for liver, bone, and diaphragm matching in mm to be 6.3, 7.8, 6.3 in M-L, 4.2, 5.8, 6.1 in A-P, and 2.5, 6.0, 3.7 in C-C directions, respectively.

Conclusions: Matching pretreatment 3D-CBCT with planning CT using the patient's liver is a feasible option showing significantly lower deviations compared to bone and the commonly used diaphragm matching. A larger PTV margin is needed when using bone and diaphragm alignment to ensure adequate target coverage in free-breathing liver SBRT.

Evaluation of a Novel Streamlined Solution for MLC-based Intracranial SRS

Everardo Flores-Martinez, Todd Pawlicki, Grace Gwe-Ya Kim

Objectives: To evaluate the planning workflow and delivery for HyperArc and to compare the results with conventional Rapid Arc stereotactic radiosurgery (SRS).

Methods: Nine VMAT plans were used to compare the plan quality and workflow for HyperArc and conventional Rapid Arc SRS. Two types of plans were created, one using an anthropomorphic head phantom and 7 clinical plans, selected for different locations, number of targets and target sizes. Four of the plans treated a single lesion plans while the other 5 treated multiple lesions. The simulation was performed on a GE CT scanner using a slice thickness of 1.25 mm. The clinical plans have been previously treated using a Varian TrueBeam linac with same beam angles (1 coplanar and 3 non-coplanar beams) and were re-planned using the HyperArc module using PO 15.6 VMAT optimization algorithm. Isocenter position, collimator angles and jaw positions were optimized using the optimizer included in the HyperArc planning module and virtual dry-runs were performed to prevent collisions. The planning strategy for conventional Rapid Arc plans included the use of control ring structures, while for HyperArc the SRS normal tissue objective (NTO) available for the Eclipse Photon Optimizer version 15.6 was used. The normalization for all plans was such that the isodose volume for 100% of the prescribed dose covered 98 % of the target volume. Patient-specific QA was performed for all plans using EPID portal dosimetry. Additionally, for two of the HyperArc plans, a phantom-based measurement was performed comparing the dose predicted by the treatment planning system with the dose measured using a pinpoint chamber and EBT XD film. QA measurements were performed on a water equivalent elliptical phantom (CIRS, model 002H5).

Results: The commissioning of HyperArc has been successfully completed from the CT-sim to the beam delivery. The IMRT factors, calculated as the ratio of the MUs to the tumor dose were 2.7±0.6 and 3.0±0.7 for the conventional and HyperArc plans, respectively. Maximum doses ranged from 126.1% to 136.9% for the original plans and from 124.5% to 168.4% for HyperArc. The conformity index (CI) for all the single-lesion plans was less than 1.18 for the original plans and 1.05 for the new plans. For multi-met cases CI values increased up to 1.89 and 1.68 for the original and HyperArc plans, respectively. The most significant difference between conventional and HyperArc plans was observed in the gradient measurement (GM), which was 0.62±0.18 for the original plans and 0.49±0.16 for the HyperArc plans. QA results of HyperArc plans using phantom based measurement and portal dosimetry passed within the department QA tolerance (3% dose/3mmDTA criteria and 10% threshold dose level). The Pass rate of Gamma test of HyperArc plans are comparable with conventional RapidArc SRS.

Conclusions: HyperArc provides a number of advantages that simplify the planning and delivery of SRS plans. The HyperArc planning module allows for automatic isocenter location, collimator angle and jaw opening simplifying the planning process especially for multiple-lesion treatments. Patient safety is ensured by means of the virtual dry-run of the treatment fields. The plan quality for HyperArc plans showed improved values of CI and GM, and higher values for the maximum dose were observed. The RTOG CI, Paddick CI and ICRU HI are included in the HyperArc plans dose statistics allowing for a more comprehensive plan evaluation.

SRS Quality Assurance Using Real-Time Optical Imaging

M. Ramish Ashraf, Petr Bruza, Benjamin Williams,
Brian W. Pogue, David J. Gladstone

Objectives: In Stereotactic body radiation therapy (SBRT) and stereotactic radiosurgery (SRS) the highly conformal dose given over 3-4 fractions requires use of small beamlets with low penumbra and a steep dose fall-off rate. It is imperative that routine QA (Percentage Dose Depth and Cross Beam Profiles), and patient specific SRS/SBRT plans QA be performed accurately. Quality assurance is currently performed using radiographic films, Ionization Chambers, Electronic Portal Imaging Device (EPID), and diode array systems. Most of these lead to a workflow which is time consuming and are limited because of spatial resolution or energy resolution inaccuracy for the most complex beamlets. In this study, we propose a remote, real-time optical imaging technique that uses a pulsed intensified CMOS camera to capture optical photons generated due to Cherenkov radiation in water tank doped with quinine sulfate.

Methods: A 140mm diameter x 305mm deep cylindrical water phantom doped with 1g/L quinine sulfate was imaged using an intensified time-gated (CMOS) camera (C-Dose, DoseOptics LLC., Lebanon, NH). The water phantom was CT-scanned and a range of static beams and dynamic plans were simulated through this in the Eclipse treatment planning system (TPS). These plans were then delivered to the phantom, from a TrueBeam linac. Static square beams of 5mm, 10mm and 50mm delivered to the phantom for initial testing. Dynamic plans included a 5mm full 360-degree arc, a head and neck VMAT and a multitarget SRS plan with couch kicks. The resulting image stacks from each experiment were analyzed both dynamically and as an average of all frames. For the static beams, the percentage dose depth (PDD) and cross beam profiles (CBP) were obtained from the averaged frame. Gamma analysis was performed on all plans relative to the TPS image data.

Results: We were able to achieve a frame rate of 10-18 frames per second (fps) for the dynamic plans. With the camera 2m away from the isocenter, a spatial resolution 0.26mm was achieved. Comparison of each experimental PDD against each TPS PDD showed that for the smallest beam sizes, 5mm, a 96.5% gamma pass rate was achieved with a 3%/3mm criteria. For the 10mm and 50mm square beams, the pass rate was 97.5% and 100% respectively. For CBP's, the 3%/3mm passing rate was 100% in the beam width region but discrepancies were seen in the penumbra region. The composite image of the 5mm 360 arc plan and the dynamic head and neck VMAT showed a 100% and 98.8% pass rate for 3%/3mm criteria, respectively. The multitarget SRS Plan with couch kicks resulted in a 93.4% pass rate for the 5%/5mm criteria.

Conclusions: Remote optical Cherenkov imaging has been demonstrated as a suitable alternative QA technique for small beamlets that are relevant in SRS and SBRT plans. Small beams near 5mm are detectable and agree well with the TPS data. QA's performed using EPID and diode arrays usually overwrite couch kicks and do not give accurate description of dose deposition, whereas in this study, the multitarget SRS plan with the couch kicks was imaged with the camera fixed to the patient frame of reference, thereby enabling us to take in to account the mechanical uncertainty of the isocenter. With 10-18 frames per second, this technique allowed us to capture data per single control point for the dynamic plans.

Disclosure of Conflicts of Interest: Brian W. Pogue is the Co-Founder, President of Dose Optics (Lebanon, NH).

Towards Application of Cone Beam CT Dosimetry (CBCT-D) to Multifocal SRS End-to-End Testing

Justus Adamson, Chibuike Umeh, William Giles, Michael Trager, Jaclyn Carrol, Suk Whan Yoon, Evan Maynard, Michelle Hilts, Andrew Jirasek, Mark Oldham

Objectives: Cone Beam CT Dosimetry (CBCT-D) is a new 3D dosimetry technique where radiation dose, recorded as a mass density change in an N-Isopropylacrylamide (NIPAM) polymer gel dosimeter, is quantified immediately following radiation delivery using on-board kV-CBCT. Here we present the ongoing efforts to develop this technique and apply it to end-to-end verification of spatial and dosimetric accuracy for multifocal SRS.

Methods: Given the relatively low contrast of the irradiated dosimeter (roughly 20-30HU), we used a low contrast phantom in order to determine the optimal kV-CBCT acquisition parameters to achieve the best image contrast and Contrast-to-Noise Ratio (CNR) for the same anode heat load. Acquisition and reconstruction parameters which were evaluated included kVp (80-120), reconstruction filter (Smooth, Standard, Sharp, and Ultrasharp), and ring suppression (Disabled, Weak, Medium, and Strong). Contrast was defined as the mean difference in signal between a target and a background ROI (each 1cm square), while CNR was defined as this difference divided by the standard deviation of the background signal.

In addition, a proof of principle end-to-end spatial analysis was carried out using a 9.5cm diameter NIPAM dosimeter: after simulation CT, a multifocal VMAT SRS plan was prepared with six 1cm diameter targets, each receiving 20Gy. The dosimeter was aligned on the treatment table using kV-CBCT guidance with 6-degrees of freedom correction after which the treatment plan was delivered. Dose information was then quantified immediately after delivery using the average of three kV-CBCTs, with total time for delivery and imaging being <30 minutes. Specialized image processing was performed to extract the dose information, which removed the background and high frequency noise. Image thresholding was used to determine the irradiated volume per target with the same volume as the prescription isodose volume.

Results: Lower kVp provided a greater contrast while higher kVp provided greater CNR given the same anode heat load. CNR was greatest for the smooth reconstruction filter and strong ring suppression. For the end-to-end test, average CNR of the delivered dose to the targets was 5.8. Centroids of each target aligned to within <2mm of the plan.

Conclusions: CBCT-D has promise as a fast & convenient method to verify delivered dose within the same frame of reference as the treatment delivery system. It is already applicable for spatial verification of multifocal SRS, and has potential to become a unique method of quantifying delivered 3D dose with high spatial resolution.

Plan Quality Control for Single Isocenter Multiple Target Radiosurgery with a Knowledge-Based Optimization Model

Yun Yang, PhD, Jun Duan, PhD, Qing-rong Jackie Wu, PhD, Guoqiang Cui, PhD, Nicole Walls, PhD, David Yoo, MD, PhD, John Kirkpatrick, MD, PhD, Fang-Fang Yin, PhD

Objectives: Single isocenter multiple target (SIMT) radiosurgery treatment with volume modulated arc therapy (VMAT) reduces treatment time significantly compared to single isocenter per target treatment. However, the treatment planning process is complicated and time consuming, and the plan quality is highly dependent on planner's experience and knowledge. In this study, a knowledge-based optimization model was created from previously treated plans and implemented for plan quality control.

Methods: Fifty SIMT VMAT treatment plans were selected to train the knowledge-based optimization model using RapidPlan (Eclipse V13.6, Varian Medical Systems). These training plans were prescribed with either one fraction (12 - 22 Gy/fx) or five fractions (5.5 Gy/fx) with 1 - 24 targets of volume ranging from < 0.1 to 116.5 cm3. Typical beam arrangements consisted of 4 - 5 partial arcs spanning 180 degrees using 6FFF energy and couch positions of 0, 45, 90 and 315 degrees. All plans were normalized to 100% prescription dose covering at least 99.5% of all planning target volumes (PTVs). The optimization model was then validated and used to assess another twenty previously treated cases. Three types of plans were created (Automatic Plan, User Plan, and Clinical Plan) for comparison. Automatic Plans started with model-predicted DVHs and went through one round of optimization without any manual adjustment. User Plans started with user-defined objectives/priorities and also went through one round of optimization. A planner then further optimized each User Plan to get the Clinical Plan. Dosimetric parameters including maximum dose (Dmax) to the organs at risk (OARs), PTV Dmax, PTV coverage, conformity index (CI), and monitor units (MU) were compared for plan evaluation.

Results: In general, knowledge-based Automatic Plans were comparable to Clinical Plans and superior to User Plans. The PTV coverage and CI in Automatic Plans were equivalent to those in Clinical Plans. Dmax for brainstem, optical chiasm, optical nerves, eyes, and lenses in Automatic Plans were lower or equivalent to those in Clinical Plans, while PTV Dmax was higher for all Automatic Plans. As a quality assurance tool, the knowledge-based model also identified two Clinical Plans with inferior plan quality. For the first identified case, all dosimetric parameters were clinically equivalent or better for Automatic Plan compared to Clinical Plan. At the meantime, the total MUs for Automatic Plan were reduced to 1477 compared to 2311 for the Clinical Plan (a 36% reduction). For the second identified case, Dmax to left optical nerve was 30% lower for the Automatic Plan, a significant reduction of 8.3 Gy. Knowledge-based Automatic Plans indicated that plan quality for both Clinical Plans could have been further improved.

Conclusions: A knowledge-based model was created for SIMT planning with VMAT technology. Results indicated that Automatic Plans generated based on the model easily met the institutional or RTOG objectives for OARs, and were comparable to manual plans in key DVH parameters for both PTV and OARs. In addition, the model based SIMT optimization process was independent of planner's knowledge and experience and substantially reduced optimization efforts since no human interaction was involved during the optimization. This knowledge-based model can be used to provide guidance for SIMT VMAT planning and also serve as a quality assurance tool to evaluate clinically treated plans.

Profile Comparisons of Small Dose Volumes between Three Radiosurgery Systems

Steve Sorensen, Dilini Pinnaduwage, Shiv Srivastava, Xiangsheng Yan, Shyan Jani, Georg Weidlich, Mohan Bodduluri, Igor Barani, Kris Smith

Objectives: To compare small field isocentric plan profiles, using full width at half maximum (FWHM), and penumbra in the x, y, z directions for the ZAP-X, Gamma Knife and CyberKnife radiosurgery systems.

Methods: The treatment planning system (TPS), for each radiosurgery device, was used to generate an isocentric plan using the smallest collimator size available. The beams were aligned with the planes of EBT3 film. The film was placed in the axial, and the sagittal/coronal orientations to capture data in all three axes. For the Gamma Knife (GK) Perfexion (Elekta, Stockholm, Sweden) a single 4 mm shot plan was created. The plan was delivered with films placed in a spherical phantom. The first delivery was with the film in the axial orientation and the 2nd with the film in the coronal orientation. For the CyberKnife (CK) system (Accuray Inc, Sunnyvale, CA) an isocentric plan was created with the head-path using the 5 mm fixed collimator. The plan was delivered to a skull phantom with film in the axial and then sagittal orientation. Finally, an isocentric plan was created with the ZAP-X (ZAP Surgical System, San Carlos, CA) using the 4 mm collimator. The plan was delivered to the same skull phantom as that used for the CK, with films placed in the same orientations. An Epson 10000XL scanner was used to scan all the films using a 48-bit color image-type and a resolution of 75 dpi. Two calibration curves were created, one using GK the other using CK. The CK curve was also used for ZAP. The optical density in the scanned films was converted to dose using these calibration curves. Dose profiles in the x, y, z direction were then plotted for each radiosurgery system. The x,y,z directions correspond to the lateral, anterior/posterior and superior/inferior directions, respectively, for a phantom placed in the head first-supine position. The FWHM and penumbra (defined as the average of the lateral width between the 80% and 20% isodose lines on either side of the central axis) were calculated. The corresponding profiles from the treatment planning systems (TPS) were extracted and compared to those measured with film.

Results: The film measured FWHM in the x,y,z directions were 6.4, 6.4, 5.1 mm for GK, 7.4, 7.4, 6.6 mm for CK and 5.8, 5.5, 5.0 mm for ZAP, respectively. The film measurements showed a penumbra of 3.3, 3.3, 1.8 mm for GK, 4.6, 4.3, 3.5 mm for CK, and 2.9, 2.9, 2.2 mm for ZAP in x,y,z. By subtracting the film measurements from the TPS values the differences between planned and delivered were quantified. For the FWHM, differences of 0.3, 0.2, 0.0 mm for GK, 0.5, 0.5, 0.1 mm for CK, and 0.0, -0.2, -0.5 mm for ZAP, were seen in x,y,z. Similarly, differences of 0.5, 0.5, 0.2 mm for GK, 0.8, 0.5, 0.1 mm CK, and -0.3, -0.2, -0.4 mm for ZAP , were seen for the penumbra in x,y,z.

Conclusions: The FWHM results show the ZAP dose volume profiles to be the smallest, followed by GK, and then CK. Acceptable agreement (FWHM < 0.6 mm, penumbra < 1.0 mm) is seen for the film measurements compared to the TPS data for all systems.

A Comparison of Intracranial Gross Tumor Volumes Generated on MPRAGE and VIBE MR Protocols

Amelia Wexler, Greg Biedermann, Joseph Cousins, Shiyang Wang

Objectives: To compare the gross tumor volume auto-contoured on Magnetization-Prepared Rapid Acquisition Gradient Echo (MPRAGE) and Volumetric Interpolated Brain Examination (VIBE) MR sequences used for stereotactic radiosurgery treatment planning.

Methods: MR imaging was performed for SRS/SRT protocol patients with two different T1-weighted post contrast isotropic imaging sequences: MPRAGE and VIBE. The order of the sequencing study was alternated to eliminate contrast timing being a confounding variable and to vary intra-study patient movement. The 1mm slice spacing was consistent between sequences. Matlab v2018a was used to auto-contour the areas of enhancement (lesion) on both studies. The localized mean separation method developed by Pang et al. (1) was used for active contouring in this study.

Results: The tumor volumes measured from MPRAGE and VIBE sequences using the non-supervised auto-contouring method were compared with manually performed treatment planning system (TPS) contours. Tumor volume measured from MPRAGE is 4.97±5.85 cm3 vs. 3.76±3.7 cm3 from VIBE. The non-supervised auto-contouring method measured tumor volume is 46%±25% vs. 40%±22% of the TPS tumor contour volume. One-way ANOVA analysis showed the p-value = 0.18, which indicates there is no significant difference between the three tumor volume mean measurements.

Conclusions: There are limited patients in the study and the brain tumors had varying primary cancers. A mix of intact and post-operative resections were analyzed. The conspicuity of the tumor affected the performance of the non-supervised auto-contouring. However, the study demonstrated that MPRAGE is in general better than VIBE in contouring the tumor volume using fully automated software with percent difference compared to the gold standard (TPS): MPRAGE 42% vs. VIBE 57%. The auto-contour method in general underestimates the treatment region compared to TPS. In some cases the MPRAGE scan time is < 2.4x VIBE scan time. This quicker scan time can contribute to the reduction in noise in the acquisitions and ultimately the interpretation and contouring.

Dose Discrepancy of External UK SRS Audit - Investigation of Planning Factors

Kirsty Blythe

Objectives: During commissioning of TrueBeam STx for use in intracranial Stereotactic RadioSurgery, in November 2016 Guys and St Thomas NHS Foundation Trust took part in a UK Cranial Stereotactic Radiosurgery Dosimetry Audit. The measured results across a number of alanine pellets within the planning target volume of an anthropomorphic phantom were +5% higher than predicted values from Eclipse. This study aimed to investigate potential reasons for this discrepancy by making systematic adjustments to the audit plan in Eclipse.

Methods: A non-coplanar 10FFF VMAT audit plan using HDMLC was generated targeting a 10cm3 PTV. Several adjustments were individually made to this original audit plan to generate different planned doses. For each change made, the dose was re-calculated with the same MU as the original plan.

These changes were: 1. Couch CT values, 2. Body contour, 3. Change to AAA algorithm from Acuros, 4. Change to High definition ROI's, 5. Use of thin IGRT couch model, 6. Reduction of couch contour, 7. Use of maximum dose to target.

The contouring of the ROI's for determining predicted dose was adjusted to assess impact on predicted dose. These changes were: A. Contouring in high definition and adjusting the size of ROI's and B. Shift location of ROI one slice (0.0625cm) superior.

Results:

1. Adjusted CT values for couch. (Interior -960MU to-1000HU, Exterior -700HUto-300HU). This resulted in a change of predicted doses by <±0.3%
2. Adjusted the body ROI to include all of the shell and apparatus. This reduced the predicted dose by ~1-1.5% throughout.
3. Used the AAA algorithm. This decreased the predicted dose to the targets by ~2.5%
4. Changed to high definition ROIs. This changed the predicted doses by up to ±0.4%
5. Changed from medium IGRT couch to thin IGRT couch. This changed the predicted dose by ~±0.1%
6. Removed 5 CT slices of couch ROI from sup end. This changed the predicted dose by ~ ±0.3%

Applying all the above effects combined decreased the predicted doses by ~1-2%.

A: Increasing (to 0.05cc) or decreasing (to 0.032cc) and contouring ROI in High Definition mode increased predicted results. The original ROIs were not created in high-def mode, and so these new ROIs are more accurate.

B: The shifted ROIs gave a mean predicted dose between ROI's predicted pellets of ~5% different from measured, with a much smaller SD between pellets (0.8% from 1.9%) The actual average dose of all the pellets has increased by ~1.7%.

Using High Definition mode when contouring, and shifting the position of ROI by one slice (0.625cm) improved the standard deviation and increased the predicted dose by 1.7%.

Conclusions: None of the Eclipse adjustments changed the predicted doses by more ~2% individually, with the exception of using AAA which decreased the predicted dose to the targets, making our predictions in worse agreement with the measurement. This may imply an issue with the density curve used in eclipse which will be investigated further.

Creating new and more accurate ROI's increased the predicted dose and shifting the ROI's one slice superior improved the standard deviation between the pellets, which is in better agreement with measured results.

These changes have not fully resolved the dose discrepancy found in the audit and so further investigation was carried out through dosimetric measurements on the TrueBeam STx which is reported on separately. Additional tuneable parameters are available in Eclipse V 15.5 which will be explored after upgrade.

Monte Carlo Commissioning for CyberKnife Multileaf Collimator and Proposed Acceptance Criteria

Tatsiana Reynolds, Mustafa Ozer

Objectives: This work aims to present Monte Carlo (MC) commissioning experience for CyberKnife (CK) Multileaf collimator (MLC). Currently there are no published data for the acceptance criteria for the MC dose calculation algorithm with MLC. Clinically measured tissue-phantom ratios (TPRs), off-center ratios (OCRs) and output factors (OFs) were compared to calculated beam commissioning data and the acceptance criteria for this algorithm were recommended.

Methods: All measurements were carried out with M6 CK Unit using the photon diode (PTW TN60018) positioned in the computer-controlled 3D Sun Nuclear Scanner. Central axis (CA) TPRs were measured for 11 field sizes (FSs) (7.6x7.7 mm2 to 115.0x100.1 mm2) at depth ranging from 0 to 300 mm. The OCRs at particular depths: 15, 50, 100, 200 and 300 mm, were calculated as the ratio of the absorbed doses at a given off-axis points relative to the dose at CA. Measurements of OCR were carried out for 11 FSs by conducting orthogonal scans across the field at a variety of depths. The OFs were defined as the ratio of absorbed dose of a particular FS relative to the dose at a FS=100x100 mm2. All measurements were made at a source-detector distance (SDD) of 800 mm.

All calculations were utilized in the Accuray Precision (Version 1.1.1.1) treatment planning system with optimum source full width half maximum of the Gaussian distribution of 1 mm and 6.7 MeV energy. Default MLC transmission settings (Center: 0.3%, End: 1.0 %, End Edge: 20%, Side Edge: 32.0%) were used for all calculations. The final calculations were performed with computation uncertainty of 0.3% for TPRs, and OCRs, and 0.2% for OFs.

Results: The measured OFs and TPRs were found to be in excellent agreement with calculated beam data. 0% difference was shown for OFs for all FSs. For TPRs, maximum percent difference between the calculated and measured TPRs was 1% for depths larger than 15 mm, and 2% in the buildup region across all FSs. To evaluate the percent difference between the measured and calculated OCRs, the beam was divided into 3 regions, within the beam (within the central 80% of the field), penumbra (dose falls off from 80% to 20%) and tail (lower than 20% of the dose). The difference between the calculated and measured OCRs were 3% within the beam, and 20%/1 mm within the penumbra. The largest observed disagreement (up to 100%) between MC calculation and measurement was observed in the tail region due to the high atomic number of the detector sensitive volume in combination with the large decrease in photon and electron energies outside of the larger beams at larger depths. The magnitude of these differences increased with increasing FS and depth.

Conclusions: This work provides the first data for the commissioning of MC with CK MLC. The acceptance criteria for the commissioning are provided.

A Beam Applicator for Radiosurgery of the Eye using a Scanning Ion Beam Delivery System

Michael F. Moyers, Wei Ren, Ying Xing, Zhuangming Shen

Objectives: Develop a method for radiosurgery of the eye using a modulated scanning ion beam delivery system (BDS).

Methods: A configurable beam applicator, beam applicator gantry, collimators, range modulator, extension cone, light field, eye fixation light, bite block, and head holder were developed to be used in concert with a horizontal proton and carbon ion beamline designed to deliver a modulated scanned beam. Since the BDS manufacturer does not allow anything to touch the BDS, the beam applicator had to be mounted onto an independent translatable gantry that moves the beam applicator into place along the beam axis during treatment. The gantry has 3 translational and 3 rotational fine adjustments to bring the devices into proper alignment with the beam and patient. The first designated use of the beam applicator was for treatment of polypoidal choroidal vasculopathy (PCV) with a proton beam. For PCV, a field of 10 mm dia¬meter was indicated with a water equivalent range of 27 mm.[1]

Results: Coincidence between the light and radiation fields was within 1 mm at the isocenter. At the center of the mesa, which coincided with the isocenter, lateral profile measurements indicated a 95% to 95% field diameter of 7.5 mm, a 50 to 50% field width of 10.6 mm, and a 80% to 20% penumbra of 1.3 mm. Propagation of uncertainties indicates the lateral alignment uncertainty to be ? 2.1 mm at the 2 s. d. level. Depth dose measurements indicated a surface dose of 53% with the 90% to 90% mesa extending from a water equivalent depth of 17 mm to 27 mm. A prescribed dose of 14 Gy(RBE), specified at the center of the mesa, can be delivered in approximately 70 seconds.

Conclusions: A method has been developed to treat a common eye disease with ion beams. To the authors' knowledge, this is the first scanning ion beam delivery system to be used for radiosurgery of the eye.

1. Moyers, M. F., Galindo, R. A., Yonemoto, L. T., Loredo, L. N., Friedrichsen, E. J., Kirby, M. A., Slater, J. D. (1999) "Treatment of macular degeneration with proton beams" Medical Physics 26(5): 777 - 782.

An Image-Guided Rotating Gamma Ray System for Intra-/Extra-Cranial SRS/SBRT

Charlie M Ma, Ahmed ElDib, Omar Chibani, Grisel Mora, Jinsheng Li and Lili Chen

Objectives: Extensive studies have demonstrated the superior dosimetric advantages of cobalt-60 beams for stereotactic radiosurgery/body radiotherapy (SRS/SBRT) of intra- and extracranial tumors compared to higher energy x-rays due to the sharper beam penumbra and the use of non-coplanar multiple source arrangement. This work investigates the potential clinical benefits of a novel rotating Gamma ray system for SRS/SBRT.

Methods: The new Gamma ray treatment system (CybeRay, OUR United RT Group, Xian, China) has a ring gantry and a focusing treatment head consisting of 16 cobalt-60 sources. Each source has 7 collimators of 6, 9, 12, 16, 20, 25 and 35mm diameter. The treatment head can swing 35˚ superiorly, allowing a total of 43˚ non-coplanar beam incident. The treatment couch provides 6-degrees-of-freedom motion compensation and the kV cone-beam CT system has a spatial resolution of 0.4mm. Monte Carlo simulations were performed to compute plan dose distributions and to compare with previously treated CyberKnife plans.

Results: The CybeRay system had a 0.5mm isocenter accuracy. The low-dose acquisition mode of the CBCT system provided real-time fluoroscopy and 3D imaging at a dose level of <1cGy. The maximum dose rate was >3Gy/min at the center of a 16cm diameter PMMA spherical phantom. The output factor varied from 1 to 0.739 for intracranial treatment using 20mm to 6mm collimators, and from 1 to 0.698 for extracranial SRS/SBRT using all 7 collimators. The beam penumbra (20%/80%) was 3.3mm and 4.5mm for the 6mm and 35mm collimators. Superior treatment plans were obtained with CybeRay for intracranial tumor ablation with much reduced near target brain doses. CybeRay also produced favorable dose distributions for peripheral lung tumors using a partial-arc technique to spare the opposite lung and critical structures.

Conclusions: The unique dosimetric properties of cobalt beams and the accurate stereotaxy/dose delivery make the new cobalt design an ideal system for advanced SRS/SBRT of intra- and extracranial targets.

The Lessons of QUANTEC Reproduced in HyTEC

Jimm Grimm, Chengcheng Gui, Matthew Deek, KiBem Kim,
Nicholas Spoleti, Chetan Bettegowda, Michael Lim,
Kristin J. Redmond, Lawrence R. Kleinberg

Objectives: To assess whether intracranial stereotactic radiotherapy results are reported using methodology sufficient to allow comparison of outcomes with varying treatment approaches. The analysis of QUANTEC was so profoundly limited by the difficulty of synthesizing results from different publications, that a QUANTEC Vision Paper (IJROBP 2010 Mar 1;76(3 Suppl):S155-60) was published to address this limitation and recommend reporting standards that would increase the utility of future studies for subsequent analysis. Unfortunately, eight years later these problems still persist in the published data, limiting the HyTEC (Hypofractionated Treatment Effects in the Clinic) effort. Here we assess the adoption of these standards and impact.

Methods: Dose, fractionation, and tumor size radiosurgery data for brain metastases were extracted from the published literature via PubMed search. Compiled data were compared radiosurgery outcomes for 150 resection cavities from our own institution. Logistic dose-response models were constructed, stratified by tumor size, histology, and fractionation as possible from the limitations of the data.

Results: A PubMed search "metastas* AND (radiosurgery OR stereotactic) AND (brain OR cranial)" on Oct 2017 returned 2,998 papers. However, only 58 of them provided sufficient details for dose-response modeling: outcomes stratified by RTOG 90-05 size criteria, prescription dose, and fractionation.

The 58 papers contained 81 usable dose / fractionation / size groups comprising 13,900 total patients. Separate models were constructed for small, medium, and large tumors, as well as separate models for 1, 3, and 5 fractions, all in terms of 1-year local control.

In our resection cavity institutional population, in terms of three-fraction equivalent 95% tumor coverage dose, minimal dose-response was observed when averaged over the entire cohort, but when stratified by size, the local control dose response of large tumors ranged from 63% at 18Gy to 71% at 25Gy, and the response of small tumors ranged from 85% at 20Gy to 94% at 30Gy. Furthermore, when stratified by histology, metastatic lung tumors did not exhibit substantial dose-response, but when also stratified by RTOG 90-05 size criteria, the response ranged from 75% to 90% local control for these tumors.

Our findings provide a potential explanation for reproducibility failure between published studies, since varying proportions of incompatible patient populations are often mixed together. Comparisons will be shown in both the published data and our own institutional cohort in terms of what can be observed and what is lost, by stratifying and combining the data, respectively.

Conclusions: Authors of clinical outcomes studies should present sufficient details of the data to enable future investigators to reproduce or refute the results. We describe important data that should be mandated for journal publication of outcomes; in particular: dose, fractionation, endpoint, technology, basic clinical information, and other pertinent information for the anatomical structures of interest should be reported per patient or at least in stratified groups.

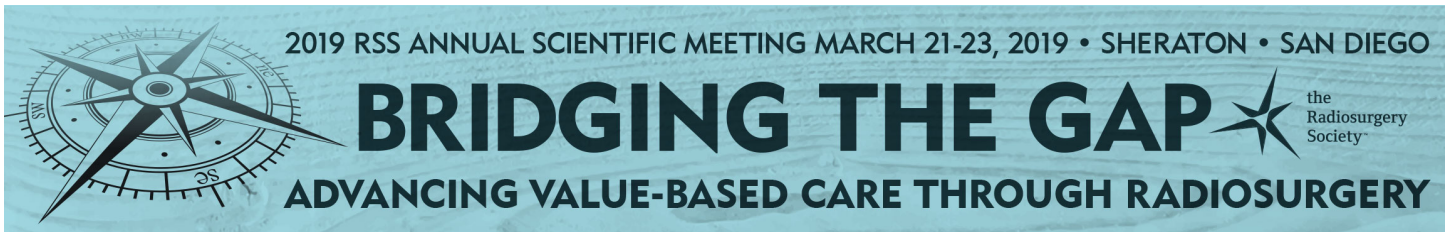

POSTER SESSION ABSTRACTS

PHYSICS

A New Approach to Small Field Dosimetry in the Robotic Radiosurgery System with Home-Made Phantom

Hasan UYSAL[1], Nihal BÜYÜKÇİZMECİ[2], Selime COŞKUN[3], Erdem UZEL[4], Mehmet Fazıl ENKAVİ[1], Şamil Osman Gürdal[3], Sait Şirin[5], Kaan OYSUL[1],

1 Medicana International Ankara Hospital / Department of Radiation Oncology
2 Selcuk University / Department of Physics
3 Radkor Dosimetry Systems
4 Radontek Medical Systems
5 Medicana International Ankara Hospital / Department of Neurosurgery

Objectives: The effective atomic number of EBT film and BeO-OSL is ~6.98 and ~7.1, respectively. The effective atomic number of human tissue is ~ 7.4. It has been demonstrated in many studies that the closer effective atomic number to human tissue is needed to acquire more accurate dosimetric results. Although its effective atomic number is not same with the human tissue, there is a wide acceptance to use EBT film dosimetric system in the practice. BeO-OSL may be a better dosimeter choice in dosimetric systems due to its effective atomic number, but there are not enough phantom studies for BeO-OSL choice. We designed a special phantom and dosimetric system in order to use the OSL dosimeter. The aim of the study is two evaluate the uncertainty in CyberKnife system using 5, 7.5 and 10mm collimators with our homemade phantom and OSL dosimeter.

Methods: A head phantom was designed and printed in a 3-D printer. In the printing process, clear resin (60-90 HU) was chosen for the soft tissues, specially prepared CaSO42H2O mixture (800-2000 HU) was chosen for bone tissues and air spaces were left empty. Special holes were created in the phantom for inserting BeO-OSL dosimeters. After acquiring CT images of the phantom, we made treatment plans using Ray-Tracing algorithm for virtual targets contoured on CT images for 5, 7.5 and 10 mm collimators using Multiplan Treatment Planing Version 4.6. The irradiation dose was prescribed as 5 Gy and it was repeated for three times. Set-up errors in irradiation were kept under 0.5 mm for translational errors and under 0.5 mm for rotational errors to irradiation same condition. After acquiring X-Ray images for set-up process, the image guidance system turned off. Pdose OSL dosimeter reader was used to measure the irradiation dose.

Results: Mean planned dose obtained from treatment planning system for 5, 7.5 and 10mm collimator was 587 cGy, 578 cGy, 583cGy, respectively and it was measured with BeO-OSL 530.5 cGy, 548 cGy, 551cGy respectively.

Conclusions: Uncertainty was increased with increasing collimator size in 5, 7.5 and 10 mm collimators. The uncertainty for the 5mm, 7.5mm and 10 mm cones was 9.62%, 5.19% and 5.48% respectively. These results were consistent with literature. The uncertainty in the small collimators in the CyberKnife system was demonstrated with a home-made phantom that was customized to the OSL dosimetry system.

A Study on Selecting Optimal Flattening Filter Free (FFF) Beam Quality for Intracranial Stereotactic Radiotherapy (SRT)

Padmanaban.V[1, 2], Dr .Sollin Selvan.K[1], Amirtharaj.G[1, 2], Dr. Srinivasan V[1], Dr. Sunitha Prabhakar[1]

1-Dept. of Radiation Oncology, MIOT International, Chennai.
2-School of Advanced Sciences (SAS), Department of physics, VIT University, Vellore.

Objectives: Use of FFF based Volumetric Modulated Arc Therapy (VMAT) for Hypo fractionated SRT (HSRT) is a well-established therapeutic modality for intracranial metastasis and benign lesions in the modern era. 6 MV-FFF and 10 MV-FFF beams available in Varian True beam STx linac offers high dose rate and increased dose per pulse which makes them an excellent choice for stereotactic treatments. As HSRT employs large dose per fraction, energy selection criteria should incorporate the impact of high and low dose gradients, integral dose and the effect of the increased Monitor Units (MU). Purpose: This study aims to critically analyse the selection of optimal beam quality for FFF-VMAT based intracranial SRT plans.

Methods: Fifteen intracranial SRT patients of different diagnose were studied retrospectively. The mean target volume was 10.46±6.73 cm3 (Range: 1.37-23.96 cm3) with dose prescription of 18 Gy to 30 Gy in 3 to 5 fractions (mean±SD: 21.7±4.01). FFF based VMAT plans were created for both 6 MV-FFF (1400MU/min) and 10 MV-FFF (2400MU/min). An attempt was made to minimize the influence of other variables by forcing both the plans with identical target coverage. All the plans were devised with 3 arcs (2 non coplanar partial arcs and one coplanar full arc with same collimator and couch angles). For both the beam quality, optimizer was driven with the clinically accepted plan constraints and dose objectives with the single hold and synchronized time in each multi resolution (MR) levels with a single intermediate calculation using Eclipse TPS (v13.6) and dose calculations were performed using Acuros XB algorithm with calculation grid size of 1.25 mm. Statistical significance was assessed for all dosimetric parameters {GIHigh, GILow, CI, MU, HI, and Beam On Time (BOT)} and OAR doses using Wilcoxon signed rank test. Results: 10 MV-FFF plans were found to have lesser MU compared to 6 MV-FFF ($p<0.002$) plans. This effect is more pronounced in deep seated tumours. 10 MV-FFF resulted in very short BOT ($p<0.0003$). No statistical significance were found in OAR doses (Brain stem ($p<0.054$), optic nerve ($p<0.779$), optic chiasm ($p<0.156$), lens ($p<0.234$) and cochlea ($p<0.28$)) between two energies. Mean Paddick CI was 1.262±0.13 and 1.257±0.12 for 6 MV-FFF and 10 MV-FFF respectively. HI was found to be 1.381±0.08 and 1.392±0.09 for 6 MV-FFF and 10 MV-FFF. Both the CI and HI were not statistically significant. We found GIHigh (V90%PI/V50%PI) was 2.9% higher ($p<0.0006$) for 10 MV-FFF and GILow (V25%PI/V50% PI) was -5.69% lower ($p<0.0006$) in 10 MV-FFF compared to 6 MV-FFF plans. Results showed that low dose volumes V2Gy and V5Gy were statistically not significant with p values <0.0648 and <0.1902 respectively. High dose volumes (V10Gy and V12Gy) showed a significant increase in 10 MV-FFF with p values <0.00064 and <0.0008.

Results: The high dose rate (2400MU/min) available with 10 MV-FFF allows the gantry to maintain maximum speed even for a large dose per fraction which in turn reduces the treatment time. Increased PDD attributed to the sparse gradient in high dose region. Reduction in number of MU's reduces the integral dose and the risk of secondary malignancy. Normal brain tissue doses were comparable between these two plans which make the 10 MV-FFF as preferable energy.

Conclusions: Adequate importance should be given for the high dose gradient region (GIHigh) when 10 MV-FFF energy is selected for intracranial SRT especially when critical organs are nearby. Results showed that increased mean energy and high dose rate of 10 MV-FFF makes it an ideal choice for VMAT based intracranial SRT.

Broadening the Clinical Applicability of Multifocal VMAT Radiosurgery to Linacs with Standard MLCs

Justus Adamson, PhD, Zhanerke Abisheva, Scott Floyd, MD, PhD, Joseph K. Salama, MD, John Kirkpatrick MD PhD, Fang-Fang Yin, PhD, Will Giles, PhD

Objectives: Stereotactic radiosurgery (SRS) of multiple brain metastases delivered via a single isocenter VMAT plan is increasingly popular. This technique delivers SRS much more efficiently compared with multiple isocenter techniques, while sparing uninvolved brain tissue, resulting in improved quality of life. This technique is primarily limited to linear accelerators equipped with high-definition MLC characterized by 2.5mm wide central leaves. Here we explore whether this technique's clinical applicability can be broadened to include standard definition (5mm) MLC leaf width. While the benefits of small MLC leaf widths (2.5mm) are well-documented for conformal radiosurgery techniques, this has not been extensively studied for VMAT. Therefore, we examined the effect of leaf width on dosimetric quality of single-isocenter, multiple target VMAT radiosurgery plans considering several methods of mitigating any dosimetric plan quality degradation caused by a wider leaf width.

Methods: 20 patients with 3-10 intracranial brain metastases originally treated with 2.5 mm MLCs were re-planned using standard 5mm MLCs. The same treatment geometry was used with 3-5 VMAT arcs with flattening filter free 6 MV photons and dose 18-20Gy in single fraction (n=16), or 5 fractions of 5-5.5Gy (n=4). Conformity index, low and moderate isodose spill (V30% and V50%) were selected for analysis and V12Gy was also analyzed for single fraction cases. Standard MLC plans were modified in several ways to mitigate the degradations of dose quality values and get similar dose quality values as in original HDMLC plans. First, VMAT arcs of the standard MLC plans were duplicated and collimator angles were shifted by 10˚, 15˚, and 90˚. Second, one and two more VMAT arcs were added to standard MLC plans and were equally spaced.

Results: When plans were re-calculated using standard definition 5mm MLCs, the MU changed from 5826±2334 to 5572±2220 (p=0.99), CI increased by 2.2%±0.04% (p = 0.98), V30% and V50% increased by 27.7%±0.15% and 20.2%±0.12% ($p < 0.01$ for both) respectively, and V12Gy increased by 17%±0.11% ($p < 0.01$). The V12Gy change did not cause sufficient concern of radionecrosis in any single fraction case to warrant fractioning treatment. Adding duplicated VMAT arcs with modified collimator angles did not improve the plan quality compared to standard MLC plans. For the standard MLC plans with one more VMAT arc, almost all dosimetric quality values improved, with the largest remaining difference being in V30%. When two more VMAT arcs were added, the percent differences further improved for all dosimetric quality values.

Conclusions: Using 5mm MLCs for single isocenter multitarget VMAT leads to minor increase in conformity index and moderate increases in low and moderate isodose spill. Among the tested methods to mitigate changes in dosimetric quality, adding two more VMAT arcs to standard MLC plans was able to give close dosimetric values as in original 2.5mm high defintion MLC plans.

Can a Jawless Ring Gantry Delivery System Provide Value-Based High Quality Intracranial Stereotactic Radiotherapy (SRT)?

Nels Knutson Jiayuan Peng Francisco Reynoso William Kennedy
Sasa Mutic Geoffery Hugo Bin Cai

Objectives: To develop a simplified, robust and standardized workflow for intracranial stereotactic radiotherapy (SRT) using a ring gantry linear accelerator equipped with a dual layer multi leaf collimator (MLC).

Methods: 10 recent clinical SRT cases treated with non coplanar volumetric modulated arc therapy to delivering 30Gy in 5 fractions on a stereotactic radiotherapy linear accelerator (linac) equipped with high definition MLCs were used to create a new planning workflow using a ring gantry delivery systems that is optimized for value based care. These re-planed cases were assessed on plan quality and deliverability, and then compared to their clinical counter parts. Each plan was created using 4 full arcs with optimized collimator rotations. A 5mm ring structure away from the planning target volume (PTV) and the normal tissue optimization were used during optimization besides the normal organ-at-risk (OAR) constraints to achieve clinical acceptable plan while maintaining a simple and standardize workflow. All plans were calculated with a 1mm dose grid and were normalized to match the clinical plan PTV coverage. For each plan, the OAR tolerances were mandatory. Conformity Index (CI), Gradient Index (GI), and Gradient Measure (GM) were then collected for all cases and compared with a matched Wilcoxon signed-rank test. All plans also underwent current clinical plan review and quality assurance protocols.

Results: With the standardized workflow, all plans were able to meet OAR constraints while matching the clinical PTV coverage. CI, GI, and GM were found to have median values vs the clinical standard of 1.1 vs 1.09 (p=0.06), 3.3 vs 2.8 (p=0.06), and 8.1 mm vs 7.1 mm (p=0.04) respectively. The interquartile range (IQR 75%-25%) were 0.1 vs clinical 0.09 for CI; 0.33 vs clinical 0.79 for GI; 2.8mm vs clinical 3.6mm for GM.

Conclusions: The simplified and standardized workflow described is useful for centers seeking to deliver intracranial SRT using a ring gantry linear accelerator in a resource thin environment.

Comparison of Two Planning Strategies for the Meningioma Stereotactic Hypofractionated Radiosurgery Planning

Slosarek K., Stapor-Fudzinska M.

Objectives: Aim of the study is to compare and evaluate two radiosurgical planning strategies using two planning systems - Precision and Eclipse with Multileaf Collimator for the meningioma treatment planning.

Methods: 15 meningiomas with maximum dimension 3 cm were used to compare two planning systems - Precision (CyberKnife M6 - Accuray) and Eclipse (Edge - Varian Medical System). In the CyberKnife System, the InCise Multileaf Collimator (MLC) was used with 82 - 2.5 mm leaves (41 pairs), and in the Varian System - HD120 MLC with 120 interleaved leaves including 64 - 2.5 mm leaves for central 8 cm field and 56 - 5 cm leaves for two peripheral 7 cm fields was used. The prescribed dose was 16 Gy in a single fraction. Treatment planning was done using the same parameters (dose constraints, auto-shells) for each system. Meningiomas were distant from organs at risk and therefore the comparative criterion was dose in the whole brain (V12 < 10cc). It will also be compared estimated treatment time, Conformity Index (CI), number of beams and total MU.

Results: Minimum, mean and maximum doses were comparable for both treatment planning systems. For the Precision System treatment time was 23 ± 3 min., there was 38 ± 4 beams, total MU were 4033 ± 819 MU, CI = 1.5 ± 0.2 and V12 = 4.2 ± 2. For the Eclipse System treatment time was 15 ± 0.5 min., there was 4 beams, total MU were 4000 ± 336 MU, CI = 1.5 ± 0.2 and V12 = 5.3 ± 1.9.

Conclusions: Treatment time is shorter for the MLC in the Varian System, but the dose distribution outside the tumor is better for the Precision System. The physician's decision is, which treatment planning strategy is better for an individual patient.

Comparison of Two Robotic Systems for the Meningioma Stereotactic Hypofractionated Radiosurgery Planning

Stapor-Fudzinska M., Slosarek K., Maciejewski B.

Objectives: Aim of the study is to compare and evaluate two CyberKnife treatment planning systems - MultiPlan and Precision, with two different collimators for the meningioma treatment planning.

Methods: 15 meningiomas with maximum dimension 3 cm were used to compare two CyberKnife treatment planning systems - MultiPlan [4.6.0] vs. Precision [1.1.1]. In the MultiPlan Planning System, a fixed collimator was used, whereas in the Precision InCise Multileaf Collimator (MLC) was used. The prescribed dose was 16 Gy in a single fraction. Treatment planning was done using the same parameters (dose constraints, auto-shells) for each system. Meningiomas were distant from organs at risk and therefore the comparative criterion was dose in the whole brain (V12 < 10cc). It will also be compared estimated treatment time, Conformity Index (CI), number of beams and total MU.

Results: Minimum, mean and maximum doses were comparable for both treatment planning systems. For the MultiPlan System treatment time was 36 ± 4 min., there was 127 ± 31 beams, total MU were 11437 ± 1093 MU, CI = 1.2 ± 0.1 and V12 = 3.1 ± 0.8. For the Precision System treatment time was 23 ± 3 min., there was 38 ± 4 beams, total MU were 4033 ± 808 MU, CI = 1.5 ± 0.2 and V12 = 4.2 ± 2.

Conclusions: Treatment time is shorter for the MLC in the Precision treatment planning system, but the dose distribution outside the tumor is better for MultiPlan and fixed collimator. The physician's decision is, which treatment planning strategy is better for an individual patient.

Feasibility of Lateral Head Flexion to Improve SRS Plan Quality for Ring Gantry Delivery

Francisco J. Reynoso Nels Knutson Geoffrey Hugo Sasa Mutic H. Michael Gach

Objectives: Ring gantry radiotherapy devices are limited to deliver beams in a single axial plane, severely limiting beam entrance angles and rendering non-coplanar beam delivery impossible. Conversely, a ring gantry geometry greatly simplifies delivery machines and increases the efficiency of treatment with the potential to decrease the overall costs of radiotherapy. This work explores the use of lateral head flexion in order to increase beam entrance angles and extend the available solid angle space for ring gantry stereotactic radiosurgery (SRS).

Methods: A 1.5T MRI scanner was used to scan seven healthy volunteers at three different head positions: a neutral position, a left lateral flexion position and a right lateral flexion position. The lateral flexion scans were co-registered to the neutral head position scan using rigid registration and extracting the rotational transformation. The head pitch, roll and yaw were computed for each registration to evaluate the natural range of motion for all volunteers. A ring gantry plan geometry was used to generate two sets of single fraction SRS plans (21 Gy/fx) for five datasets: one coplanar set for head neutral scans, and a three arc path set using the head neutral and lateral head flexion scans. The conformity index (CI), gradient measure (GM), R50, and R10 were used to evaluate both sets of plans.

Results: The average roll, pitch and yaw was 16.9˚±3.7˚, 4.1˚±4.7˚, and 2.54˚±4.9˚ for right lateral flexion and 14.0˚±3.7˚, 4.9˚±4.3˚, and 2.8˚±5.4˚ for left lateral flexion. The CI decreased an average of 8.7% from 1.32 on the head neutral plans to 1.20 on the lateral head flexion plans. The GM decreased 9.2% from 5.3 mm to 4.9 mm, R50 decreased 6.9% from 3.72 to 3.46, and the R10 decreased 29.1% from 62.3 to 44.2.

Conclusions: Lateral head flexion was shown to increase beam entrance angles considerably improving plan conformity and normal tissue sparing in this pilot study of five sets of plans. Rigid registrations demonstrated each lateral flexion to be analogous to a 15˚ couch kick. The quality of SRS plans delivered on ring gantry radiotherapy devices may significantly improve with the use of a lateral head flexion setup.

Investigation of the Suitability of the MAGIC Polymer Gel Dosimeter for Small Field Dosimetry

Mehmet Fazil Enkavi, Mustafa Cengiz, Mete Yeginer

Objectives: Dosimeters with having small sensitive volume and tissue-equivelancy are preffered in small field dosimetry. These dosimeters are generally ion chambers, solid-state dedectors which is giving point dose information and providing 2D dose distrubition, such as film dosimeters. The only dosimeter that providing 3D dose distrubition is gel dosimeters. The purpose of this study was to investigate MAGIC polymer gel dosimeter for small field dosimetry.

Methods: In this study, MAGIC (Methacrylic and Ascorbic acid in Gelatin Initiated by Copper) polymer gel dosimeters were fabricated. Using with CyberKnife robotic radiosurgery treatment device and its 5, 7.5, 10, 12.5, 15, 20, 25, 30, 60 mm collimators, small field measurements taken by microDiamond dedector, SRS Diode dedector, PinPoint ion chamber, Gafchromic and MAGIC polymer gel dosimeter. Beam profiles at 15, 50, 100 mm depth and percent depth dose, relative dose factors are measured with all dosimeters. Penumbra widths, full width at half maximums, maximum dose depths and relative dose factors of MAGIC polymer gel dosimeter compared with other dosimeters and suitability of gel dosimeter is investigated. MR images of gel dosimeters are taken with 1.5T MRI device, at TR 4040 ms and TE 50-100-150-180ms with 1.5 mm slice thickness and 0.34 mm pixel size. MR images analyzed with PolyGeVero software.

Results: PDD and output factors were found compatible with microDiamond and SRS diode detectors. The maximum dose points for SRS diode and microDiamond detectors were found within 1 mm difference. When penumbra, FWHM and beam flatness values were compared with all other dosimeters, unacceptable differences were observed. MAGIC polymer gel dosimeter FWHM values showed an expansion from all other dosimeters at a depth of 15 mm, and a narrowing at a depth of 100 mm.

Conclusions: The polymer gel dosimeters should be cautiously used in small areas due to incompatibility with the reference dosimetry results and uncertainty it has.

Obtaining Submillimeter Targeting Accuracy for Lung Tracking during End-to-End Testing of a Robotic Radiosurgery System

Joshua James MS, Zachary Carter MS, Bill Vogel BA RT(T), Brian Wang PhD

Objectives: It is desired to have submillimeter targeting accuracy during robotic radiosurgery, even when tracking moving lung tumors. End-to-end (E2E) testing is used to verify the system's ability to achieve this level of accuracy. The treatment planning system for Accuray's CyberKnife system is able to automatically center the calculated dose distribution on the target for the purpose of E2E testing. In its most recent software version, Precision 1.1, the treatment planning system is only able to center the dose distribution calculated using the ray tracing algorithm. The ray tracing algorithm's inaccuracy within lung tissue causes the calculated dose distribution to be centered incorrectly resulting in a failed E2E test (targeting error > 0.95mm). The purpose of this study is to present a manual method of centering the dose distribution on the target using the Monte Carlo algorithm in order to obtain the desired submillimeter targeting accuracy during E2E testing of Xsight lung tracking.

Methods: Isocentric treatment plans were created on an anthropomorphic thorax phantom using the standard E2E automated workflow that centers the ray tracing generated dose distribution on the target. The dose distribution was then recalculated with the same beam geometry using the Monte Carlo algorithm, and a contour was created from the appropriate isodose surface. The difference in coordinates between the centroid of the contoured isodose surface and the centroid of the target was used to calculate the necessary shift in isocenter position to align the two centroids. Both the shifted and nonshifted isocenter plans were delivered to the moving thorax phantom (3cm of motion in the sup/inf direction) using CyberKnife's Xsight Lung tracking. Film placed inside the target volume was analyzed to determine the actual difference between the centroid of the target volume and the measured dose distribution, which is a measure of the targeting accuracy of the system. This process was repeated 3 times for both the fixed and iris collimator.

Results: The isocenter shift needed to center the Monte Carlo generated dose distribution on the target was 0.4mm anteriorly and = 0.1mm in the left/right and sup/inf direction. The primarily anterior shift is due to the beams transversing a greater length of lung equivalent material in the ant/post direction and the asymmetry of the beam geometry in the ant/post direction. The average total targeting error for the nonshifted and shifted E2E plans delivered to the phantom was measured to be 1.12 and 0.84mm, respectively for the fixed collimator and 1.04 and 0.83mm, respectively for the iris collimator. As expected, the largest difference in targeting accuracy was in the ant/post direction, where the targeting error decreased for the fixed and iris collimators by 0.39 and 0.47mm, respectively.

Conclusions: The ray tracing algorithm is insufficient for accurately calculating dose distributions in the lung and leads to failing results of E2E testing of Xsight lung tracking on the CyberKnife system. Therefore, a manual method of creating E2E treatment plans using the Monte Carlo algorithm has been presented. Using this method, we were able to verify the submillimeter targeting accuracy of Xsight lung tracking on the CyberKnife system with total targeting error results ranging from 0.75 to 0.95mm.

Reporting Radiosurgery Plan Indices Must Be Accompanied by the Derived Method as Some Indices Can Vary Significantly with Technique used for the Same Definition - Case Study, The High Dose Spillage as used in Several RTOGs

Roland Teboh Forbang, PhD; Brett Lewis, MD, PhD; Alois Ndlovu, PhD

Objectives: Radiosurgery indices, useful in evaluating SRS/SRT/SBRT plan quality are derived from a treatment plan based on a given definition. However some derived indices may vary based on the method used even though the correct definition was applied. We illustrate this using the High Dose Spillage (HDS) that is required in several RTOG protocols, for example, RTOG 0813, and RTOG 0915.

Methods: We utilized clinically approved treatment plans of eight (n=8) previously treated lung SBRT patients. For each plan, we computed HDS, defined as the volume of tissue outside the PTV, expressed as a percentage of the PTV volume, irradiated by at least 105% of the prescribed dose (1.05Rx). We used 2 techniques (T1, T2) to compute HDS in each patient case; T1: HDS = (All Tissue Volume receiving at least 1.05Rx) MINUS (PTV Volume receiving at least 1.05Rx). The External (or Body) contour is used for all tissue. T2: First we used the treatment planning system (TPS) to derive a new contour, namely the external contour MINUS the PTV (External-MINUS-PTV), then HDS = Volume of External-MINUS-PTV contour receiving at least 1.05Rx The HDS as derived from T1 and T2 were then compared.

Results: The derived HDS as calculated from the 2 techniques was consistently different among all 8 cases. On average, we observed a 90% ± 13% (range, 65% to 100% discrepancy) between T1 and T2. Furthermore, depending on the method used in deriving the new contour in T2, the resulting HDS calculated was different. For example, when we used (a) deriving the new contour using margins, where the new contour is derived from the External contour with zero margin and using the PTV as an avoidance structure versus (b) using the Boolean functionality in the TPS where the new contour was derived by applying External sub PTV. We observed a 21% discrepancy in calculating HDS between (a) versus (b) for one patient. We used Varian Eclipse TPS, version 11.The observed differences in HDS can be attributed to volume round-off errors which may not be significant with respect to the final derived volumes but does have an effect in the calculated HDS as shown. For our clinical evaluations, we use ClearCheck (RadFormation Inc, NY) to compute the indices including HDS for our SBRT plans. The ClearCheck results are in agreement with those calculated in T1.

Conclusions: This work shows that important quality indices used in evaluating SRS/SRT/SBRT plans may be different depending on the method of derivation. Therefore when reporting or requesting these indices, it is important to clearly state how the indices are derived from the treatment plans, something which is currently lacking in current protocols including RTOGs.

Single Center Study of Clinical Dosimetry Data Characteristics and Quality Assurance of Robotic Radiosurgery

Jianping Zhang, Lin Wang, Benhua Xu, Xiaobo Li, Miaoyun Huang, Yuangui Chen

Objectives: The clinical dosimetry data characteristics and quality assurance commissioning procedure of VSI Cyberknife was studied in this research.

Methods: Combining the practical operating experience, a comparative analysis was carried retrospectively on clinical reference data supplied by Accuray Incorporated and the clinical commissioning data of VSI Cyberknife which installed in our center in July 2017. Except for off-center ratios, the clinical dosimetry data were measured used by PTW 60019.

Results: It was pointed out that the analysis of Auto quality assurance and End-to-End test should balance of its eccentricity, three-dimensional error and the total radial error. Both radiochromic film and equivalently high spatial resolution detector could be used for Iris QA, but the use of radiochromic film was strongly recommended when the baseline set of measurement was done. At 650mm, 800mm and 1000mm SAD, the average deviation between measurements and reference value for output factors across all Fixed size cones were -1.27%, -0.21% and 0.70%, respectively. And for 5/7.5 mm collimators, the values were -5.10%/-2.67%, -2.08%/-1.41% and -1.12%/0.06%, respectively. For Iris apertures, the values were -1.88%, -0.74%,0.09%, -8.61%/-3.53%, -4.38%/-1.97% and -1.34%/-0.33%, respectively. At the surface of water, the mean value of tissue phantom ratios of two types of collimator were -6.22% of Fixed vs -4.81% of Iris, respectively, both less than reference values. Except for 5mm and 7.5mm Iris collimators, the measurement curves of off-center ratios for those two types of collimators had a tendency that the shoulder and bottom of curves toward positive deviation, and the deviation was more obvious with the increase of collimator sizes. The output of dose calibration for IAEA TRS 277 was about two percent smaller than that of TRS 398.

Conclusions: In acceptance procedure of Cyberknife, the characteristics of two types collimators especially for smaller collimators should be considered adequately, the user should choose the appropriate commissioning procedures.

Stereotactic Cone Commissioning for Flattening Filter Free Photons of a Linear Accelerator using a Plastic Scintillator Detector

S. Crawford, T. Law, W. Snyder, J. Wei

Objectives: To describe a practical method of cone commissioning using a plastic scintillator detector (PSD) and diode detector and present the data for public reference.

Methods: Measurements were performed with a 1mm x 3mm PSD and a 0.8 mm x 0.8 mm diode detector. Though the properties of PSD make it ideal for small field measurements, several challenges in its implementation had to be overcome. A custom 10 cm thick Cerrobend shield was used to minimize the effect of radiation incident on the photodiode component of PSD. A plastic c-clamp sleeve was used to protect the PSD sheath, allowing it to be mounted using standard chamber attachment accessory. CLR calibration was performed in water with PSD parallel to incident beam, following vendor recommended procedure. Maximum irradiated fiber condition was met by attaching a small weight to the fiber, keeping it submerged at a stable depth, while the minimum fiber configuration was achieved by pulling excess fiber out of the water. PSD centering was performed by acquiring a measurement at nominal beam center by the light field and determining the positions of the in-plane and cross-plane 50% signal through linear interpolation. The depth of measurement was determined with the vendor-provided cap with a white line indicating the effective POM. Output factors (OF) were measured for 6X-FFF and 10X-FFF photons and all cone sizes (4, 5, 7.5, 10, 12.5, 15, and 17.5 mm) with the PSD and diode detector at 95 cm SSD, a depth of 5.0 cm, and jaw setting of 5 cm x 5 cm. A daisy-chain correction was done with a 0.125 cc ion chamber at a junction field of 4 cm x 4 cm for both PSD and diode. TMR curves were measured up to 21 cm using the TPR acquisition package and a diode. TMR point checks were performed with the PSD. Depth dependent correction factors, determined through a linear fit, were applied to the TMR curves so that a close match to the PSD point data was achieved. End-to-end test was conducted for the 4 to 10 mm cones with a head phantom and triple channel films.

Results: PSD measured OFs for 6X-FFF were 0.576, 0.633, 0.725, 0.781, 0.817, 0.843, and 0.859 for 4 to 17.5 mm cones, respectively; for 10X-FFF, 0.484, 0.547, 0.656, 0.730, 0.784, 0.823, and 0.852. Diode detector measured OFs for 6X-FFF were 0.608, 0.668, 0.754, 0.798, 0.826, 0.846, and 0.859 for 4 to 17.5 mm cones, respectively; for 10X-FFF, 0.511, 0.582, 0.695, 0.763, 0.811, 0.844, and 0.868. The PSD OFs agree with Monte Carlo simulations by Cheng et al 2016 within 2.5% for both energies. Diode OFs agree with the vendor representative data within 1.0% and 1.5% for both energies. Differences in OFs as measured by diode and PSD range from 0.5% to 6.5% for various cone sizes, which is consistent with data reported by Franceson et al in 2014 and Tanny et al in 2015. PSD TMRs at 10 cm depth for 6X-FFF (normalized to d=1.5cm) were 0.594, 0.602, 0.614, 0.623, 0.629, 0.636, and 0.641 for 4 to 17.5 mm cones, respectively; and for 10X-FFF (normalized to d=2.5cm), 0.693, 0.697, 0.711, 0.719, 0.726, 0.733, and 0.739. Diode TMR at 10 cm depth for 6X-FFF were 0.588, 0.599, 0.612, 0.616, 0.626, 0.628, and 0.635 for 4 to 17.5 mm cones, respectively; and for 10X-FFF, 0.687, 0.696, 0.708, 0.716, 0.725, 0.729, and 0.738. Film gamma analyses yielded passing rates of 97.5% to 99.3% for 4 to 10 mm cones at 1% and 1 mm with a 10% threshold.

Conclusions: With proper care, PSD is an accurate and practical tool for commissioning small fields, including stereotactic cones.

The Radiotherapy Methods Study and Short Term Effect for the Preservation of Bilateral Ovarian Function during Radiotherapy for Cervical Carcinoma

Cheng Xiaolong, Liu Jiping

Objectives: To explore the radiotherapy methods of bilateral ovarian function protection during radiotherapy for cervical cancer based on linear accelerator (intensity modulated radiation radiation therapy (IMRT), volume modulated arc therapy (VMAT) and Helical Tomotherapy (HT).

Methods: A total of 10 young cervical cancer patients in stage IA~IIB with cervical cancer radical double lateral ovarian transposition and radiotherapy in Zhejiang Cancer Hospital during the period of January 2016 to August 2018 were enrolled in this study. The radiotherapy treatment plans of lowering the dose to the ovary, including IMRT,VMAT and HT with a prescribed dose of 45Gy at 1.8Gy per fraction. Dosimetric differences in PTV,ovary,bladder,rectum,bowel bag,spinal cord,bone marrow,femoral head were compared. The dosimetric advantages of preserving unilateral ovarian plans were compared,and the application of three dimensional conformal radiation therapy (3D-CRT) technology was also tried to apply on preservation of ovarian function.

Results: The mean volums of PTV, left and right ovaries, the recent average distance to the PTV edge and lliac crest were (1065.02±145.33)cm3, (13.12±6.52)cm3, (13.52±6.04)cm3,(3.40±1.23)cm, (3.70±0.83)cm, (-0.87±2.21)cm, and (1.11±2.41)cm, respectively. The HT technology could reduce the max dose mean dose of left and right ovaries, the max dose of PTV, homogeneity index,bladder V20,V30 and V40, bowel bag V40, bone marrow V20, max dose of spinal cord ,which were (383.50±68.68)cGy, (309.80±66.34)cGy, (246.70±51.09)cGy, (196.90±52.40)cGy, (4901.00±91.76)cGy, (0.092±0.028), (89.22~100)%, (43.35~100)%, (19.59~69.54)%, (13.06~35.64)%, (46.1~63.1)%, (3105~3905)cGy, compared with IMRT and VMAT, and these differences were statistically significant (P<0.05). IMRT fad an advantage in the minimum dose limit of PTV at (4374.00±30.36) cGy, and other dosimetry parameters were worse than HT, but better than VMAT. The plan of protecting unilateral ovarian function was not achieved to reduce the ovarian dose and optimize the distribution of PTV and organs at risk. 3D-CRT was inferior to IMRT, VMAT and HT in limit ovarian dose and PTV conformal index, which was only applicable for cases with the upper margin of PTV below lumbar vertebrae 5 due to the limit of spinal cord tolerance dose. The ovarian dose limit (Dmax<4Gy, Dmean<3Gy) and the prejudging method of whether the ovarian function could be protected when radiotherapy for cervical cancer was proposed (the ovary is 2.5cm away from the edge of PTV, and the lower edge of the ovary is higher than the iliac ridge).

Conclusions: Compare with IMRT, VMAT and 3D-CRT, HT can reduce the maximum dose of the ovaries, and ensure that PTV and other organs at risk have a good dose distribution. The treatment cost and equipment requirements of HT technology are relatively high. The IMRT technology with special field can be recommended if conditions are not allowed. 3D-CRT technology has certain requirements on the PTV range and its application needs to be confirmed by further research.